Patterned Colloidal Deposition Controlled by Electrostatic and Capillary Forces

Patterned Colloidal Deposition Controlled by Electrostatic and Capillary Forces

Joanna Aizenberg, Paul V. Braun,* and Pierre Wiltzius
Lucent Technologies, Bell Laboratories, Murray Hill, New Jersey 07974
(Received 14 October 1999)

We use substrates chemically micropatterned with anionic and cationic regions to govern the deposition of charged colloidal particles. The direct observation of the colloidal assembly suggests that this process includes two steps: an initial patterned attachment of colloids to the substrate and an additional ordering of the structure upon drying. The driving forces of the process, i.e., screened electrostatic and lateral capillary interactions, are discussed. This approach makes it possible to fabricate complex, high-resolution two-dimensional arrays of colloidal particles.

PACS numbers: 82.70.Dd

Topographically complex surfaces with submicron periodicities are of growing importance since they provide routes to the fabrication of highly oriented colloidal crystals, biologically active substrates, and optical and electronic devices [1–3]. Direct control of the spatial distribution of micrometer scale objects across large areas is, however, very difficult. Understanding of the fundamental mechanisms that drive the assembly of particles at the micrometer scale will bring about new strategies for the fabrication of well-ordered arrays of micron-size objects.

Colloidal particles are interesting and versatile building blocks for the generation of two- (2D) and three-dimensional (3D) microstructures [4]. Because of their nearly monodisperse nature, colloidal particles can self-assemble into long-range lattices when appropriately settled or dried out of their supporting solvent [5,6]. Self-assembly alone is, however, greatly restricted to the formation of *close packed* 2D and 3D arrays of colloidal particles and does not lead to more complex patterns. A certain degree of control over colloidal self-assembly has been achieved through external electric [7] or intense optical fields [8] and by manipulating the interaction potential [9]. A more promising approach is colloidal epitaxy; that is, the deposition of colloidal particles onto a patterned (e.g., lithographically modified [1]) substrate. Recently, microcontact printing (μCP) was developed as a simple and powerful method for micron-scale chemical patterning of surfaces [10]. Using this technique, μ-patterned self-assembled monolayers (SAMs) of functionalized alkanethiols can be routinely generated over large areas on metal substrates. Patterned SAMs were shown to control various area-selective processes [2,10,11].

Here we describe a new approach to colloidal epitaxy that exploits SAMs μ-patterned with ionic regions as templates for the deposition of charged colloidal particles. The colloids used in this study consisted of polystyrene spheres suspended in distilled water at volume fraction of $\sim$4%. We have chosen negatively charged carboxyl-terminated spheres with a diameter of 1.11 μm $\pm$ 1.8% and $N = 3.52 \times 10^6$ charges/particle, and positively charged amidine-terminated spheres with a diameter of 1.03 μm $\pm$ 7.1% and $N = 2.45 \times 10^6$ charges/particle. To prepare substrates, glass coverslips were coated with 2 nm of Ti and 20 nm of Au. Patterned SAMs were formed using μCP as described elsewhere [10]: elastomeric polydimethylsiloxane (PDMS) stamps with various relief structures were "inked" with a 10 mM solution of $HS(CH_2)_{15}CO_2H$ in ethanol, brought into conformal contact with gold for 10 s, and then rinsed with ethanol; the noncontact areas were derivatized with a 10 mM solution of either $HS(CH_2)_{11}N(CH_3)_3{}^+Cl^-$ or $HS(CH_2)_{15}CH_3$ in ethanol by immersion for 1 min (Fig. 1). The μ-patterned substrates bearing anionic and cationic regions ($-/+$ templates) or anionic and neutral regions ($-/n$ templates) were supported upside down in a colloidal suspension to avoid the nonspecific sedimentation induced by gravity. After 2 min, the substrates were removed, and the excess suspension was carefully rinsed from the surface. The wet substrates with the deposited colloidal particles were placed under the light microscope

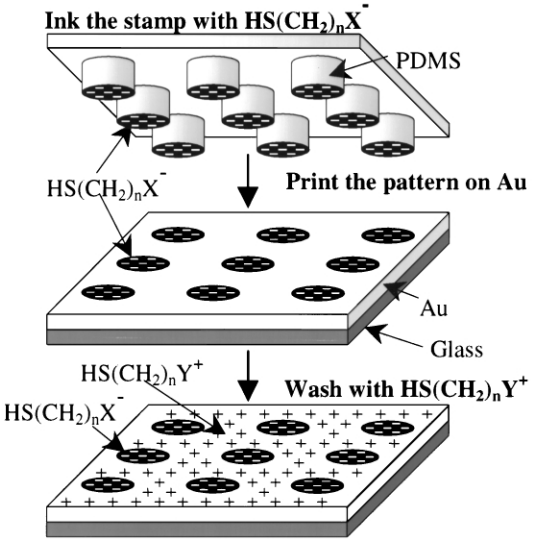

FIG. 1. Schematic presentation of the fabrication procedure of a substrate chemically patterned with anionic and cationic regions using μCP.

and the dynamics of colloidal assembly was monitored in real time as the samples were allowed to dry.

For the $-/n$ templates, the charged colloidal particles preferentially interacted with the oppositely charged regions of the μ-patterned SAM, but occasional adsorption to the neutral regions also occurred, presumably, due to hydrophobic interactions between methyl-terminated SAM and polystyrene spheres. A much greater selectivity was observed for $-/+$ templates. Figure 2 shows an example of a high-resolution 2D array of colloidal particles. The template consisted of a square array of well-resolved negatively charged circles of diameter $d = 5.6$ μm and of periodicity $p = 10$ μm in a positively charged background (Fig. 2 inset). The deposition of *positively* charged particles from the suspension occurred entirely on the negatively charged regions of the SAM with a highly uniform distribution, 6.1 ± 0.6 spheres per circle [Fig. 2(a)]. When *negatively* charged particles were deposited onto the same substrate, a grid pattern formed [Fig. 2(d)]. The average distance between the centers of adjacent particles (l_a) in wet samples determined using image analysis of the micrographs was 1.8 ± 0.3 μm. At the last stage of water evaporation, when the thickness of the water layer became comparable to the particle size (detected from the appearance of Newton fringes), the attached colloids rearranged. The particles within each negatively charged region moved towards the centers of the circles and formed dense clusters [Fig. 2(b)]. Figure 3 shows the overlaid distribution of the adsorbed particles within a total of 30 superimposed circles mapped for a region of 50×60 μm^2 in a wet and dry sample. It demonstrates that focusing occurred towards the centers of the circles even for the wet samples: 95% of spheres were excluded from the edges of the patterned regions by about $l \sim 0.65$ μm [Fig. 3(a)]. In the dried sample, the size of the depletion region increased to ~ 1.1 μm [Fig. 3(b)].

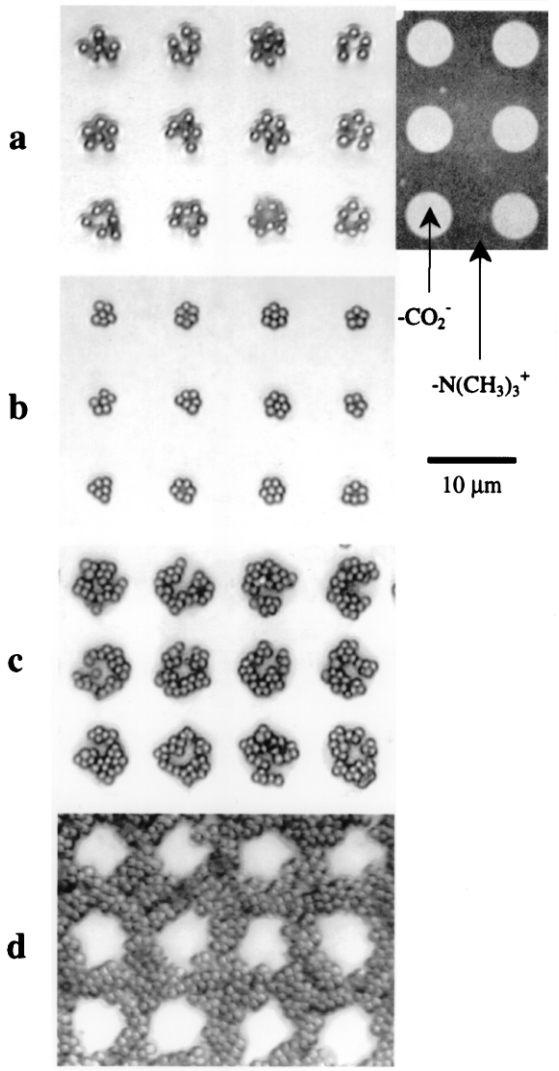

FIG. 2. Light micrographs showing localized deposition of charged colloidal particles controlled by a μ-patterned ionic SAM. The inset presents a scanning electron micrograph of the geometry of the substrate. (a) Specific attachment of positively charged spheres to the negatively charged regions of a template (wet sample). (b) The same region as in (a) showing further focusing of the structure after drying. (c) Deposition of positively charged colloids from a 0.005M LiCl solution. (d) Specific attachment of negatively charged spheres onto positively charged regions of the μ-patterned surface.

These observations strongly support a two-stage mechanism of colloidal assembly. During the first stage, patterned colloidal deposition driven by long-range electrostatic forces occurs [4,12]. Neither short-range hydrogen bonding nor acid-base reactions between amidine-terminated spheres and carboxyl-terminated regions of SAMs can drive the spheres away from the interface between the SAMs over submicron distances. The mechanism of the deposition of positively charged colloids on a $-/+$ template is schematically illustrated in Fig. 4(a): (i) particles in the vicinity of the positively charged regions are repelled from the substrate (f_r); (ii) particles in the vicinity of the negatively charged regions undergo attraction (f_a) and attach to the substrate; (iii) particles at the interfaces between the two regions undergo both

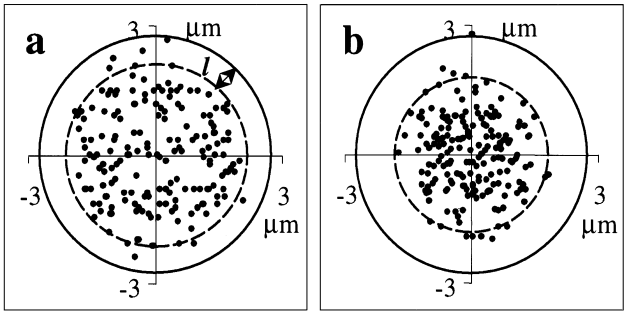

FIG. 3. Graph showing the superposition of 30 negatively charged regions of the substrate with positively charged colloids adsorbed on them. The data correspond to the experiments shown in Figs. 2(a) and 2(b). Solid circles represent the border of the negative regions; the dashed circles correspond to the area occupied by 95% of the particles; the dots represent the centers of the spheres. (a) Wet sample with the depletion zone shown. (b) Dry sample in which additional focusing has occurred.

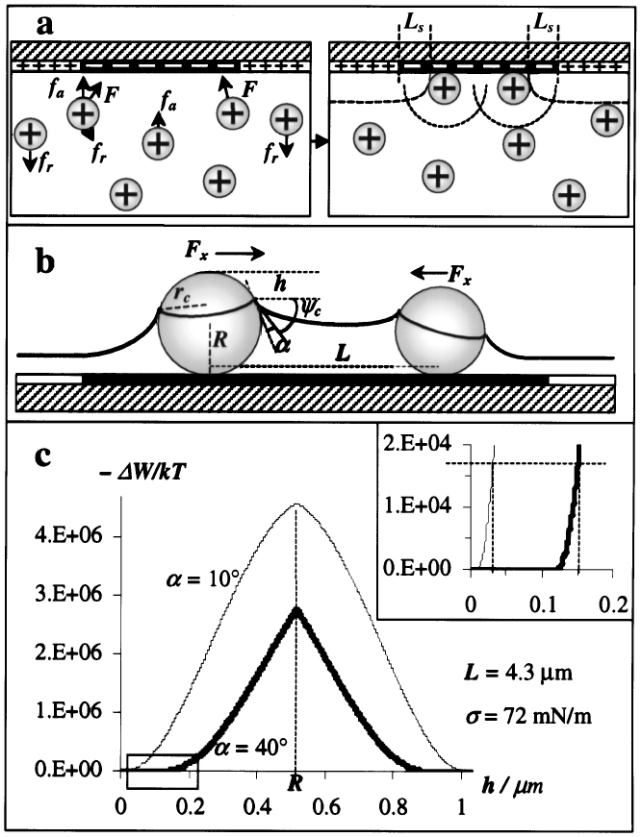

FIG. 4. Schematic presentation of the two-stage mechanism of colloidal assembly on a μ-patterned ionic substrate (see text for details). (a) Specific deposition driven by screened Coulomb interactions. (b) Focusing of the structure due to lateral capillary attraction (adopted from [5]). (c) Energy of capillary interaction as a function of the receding of the liquid layer.

the repulsion from the cationic SAM and attraction to the anionic SAM and are, therefore, driven away from the interfaces ($\boldsymbol{F} = \boldsymbol{f_r} + \boldsymbol{f_a}$) and attach towards the centers of the negatively charged regions. The depletion region (l) [Fig. 3(a)] will then originate from the screened length in Coulomb interactions (L_s) [Fig. 4(a)]. We estimate the corresponding energy [Eq. (1)] of electrostatic interaction between the particles and surface using a linear superposition approximation [13]:

$$\Delta V \sim \varepsilon \Psi_1 \Psi_2 (a_1 a_2 / L) e^{-\kappa(L - a_1 - a_2)}, \qquad (1)$$

where ε is the dielectric constant of the medium, Ψ_1 and Ψ_2 are the surface potentials of the interacting particles, a_1 and a_2 are the radii of the interacting particles, $L = a_1 + a_2 + h$ is the distance between the spheres, and $1/\kappa$ is the characteristic Debye-Hückel length. For amidine-terminated particles, $a_1 = R = 0.515 \times 10^{-6}$ m and the charge density $N_s = N/4\pi R^2 = 7.35 \times 10^{17}$ charges/m^2. A simple dissociation model [14] predicts the maximum surface potential Ψ_1 for this surface charge in dilute electrolyte solutions to be about 120 mV. For the SAM surface, $a_2 = 1$ m $\gg a_1$ (the surface is practically flat) and the charge density $N_s = 5 \times 10^{18}$ charges/m^2. The corresponding surface potential Ψ_2 is approximately -130 mV [14]. For small separations ($h \to 0$),

$$\Delta V \sim -7 \times 10^{-17} \text{ J}, \quad \text{or} \quad 1.7 \times 10^4 \text{ kT}.$$

The importance of electrostatic forces in directing patterned colloidal deposition was further supported by the experiments in which colloidal suspension containing 5 mM LiCl solution was allowed to assemble on a $-/+$ template. The addition of salts suppresses Coulomb interactions, decreasing L_s [4]. Consistently, the spheres populated the whole area of the oppositely charged circles [Fig. 2(c)].

The second stage of colloidal assembly corresponds to the rearrangement of particles that occurs during drying. We believe that this process originates from attractive capillary forces appearing between particles partially immersed in a liquid layer [5] [Fig. 4(b)]. Similarly to the flotation capillary forces [12], immersion capillary attraction arises from the deformation of the liquid surface and the induced asymmetry of the contact line at the surface of the particle. It has been suggested [5] that the free energy of capillary interaction can be expressed by Eq. (2):

$$\Delta W \sim 2\pi\sigma r_c^2 (\sin^2 \Psi_c) R/(L - 2R), \qquad (2)$$

where σ is the surface tension, $r_c = [h(2R - h)]^{1/2}$ is the radius of the contact line at the surface of the particle, $\Psi_c = \arcsin(r_c/R) - \alpha$ is the mean slope angle of the meniscus at the contact line, L is the distance between the particles, and α is the contact angle [Fig. 4(b)]. The measured contact angle for amidine-terminated particles in water was $\alpha \sim 40°$. The maximum energy of capillary interaction corresponds to the minimum $L = l_a = 1.8$ μm:

$$\Delta W \sim -5 \times 10^{-14} \text{ J}, \quad \text{or} \quad 1 \times 10^7 \text{ kT}.$$

These values are significantly higher than those obtained for electrostatic energy. The energy of interaction between the most remote particles ($L = d - 2l = 4.3$ μm) as a function of the receding of the liquid layer (h) is shown in Fig. 4(c). The focusing of the attached particles starts when the energy of capillary attraction exceeds the energy of electrostatic interaction. This corresponds to a minor receding of the liquid layer: $h = 150$ nm and 30 nm for amidine-terminated ($\alpha \sim 40°$) and highly carboxylated ($\alpha \sim 10°$) colloidal particles, respectively [Fig. 4(c), inset]. Moreover, no notable difference in the particle reassembly occurred upon the addition of electrolytes, supporting the conclusion that the effect of Coulomb interactions at the second stage is insignificant.

The combination of electrostatic and capillary forces can be further used to control the fabrication of ordered 2D patterns of *single* colloidal spheres. Figure 5(a) shows a sample array of positively charged 1 μm spheres formed on a $-/+$ template composed of a square array of negatively charged circles of diameter $d_1 = 2.9$ μm and of periodicity $p = 10$ μm. The location of spheres is significantly focused in the centers of each circle: after drying, the distance from the center, $\Delta x < 0.25$ μm for 95% of particles [Fig. 5(b)]. The rationale for the experiment is schematically presented in Fig. 5(c). As discussed above,

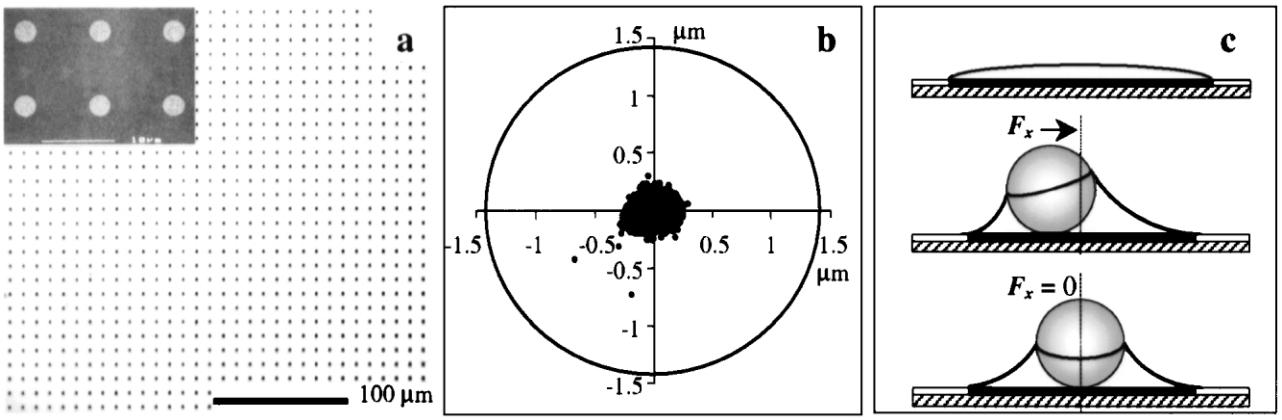

FIG. 5. Fabrication of ordered 2D arrays of single colloidal particles. (a) Light micrograph of a sample array; the inset shows a SEM of the template structure. (b) Mapped distribution of particles demonstrating a high degree of focusing within the outlined circle. (c) Schematic presentation of the proposed mechanism of particle ordering.

the first stage includes the patterned deposition of colloids driven by electrostatic forces. When the diameters of features in a μ-patterned SAM (d_1) lie in the interval

$$1.3\ \mu\text{m} = 2l < d_1 < 2l + l_a = 3.1\ \mu\text{m},$$

where $l = 0.65\ \mu$m is the size of the depletion region estimated in Fig. 3(a) and $l_a = 1.8\ \mu$m is the average distance between adjacent deposited particles, screened Coulomb interactions will allow the attachment of only one sphere to each circle at the distance from the center $r_x < d_1/2 - l$. The mechanism of the ordering at the second stage is somewhat different from the lateral capillary attraction that develops between two adjacent particles partially immersed in liquid. Control experiments in the absence of colloids showed that the last drops of water are pinned by the printed regions in the SAM [Fig. 5(c), top], presumably due to a higher density of defects in a printed SAM relative to a SAM adsorbed from solution [15]. The presence of a particle off center in this region will cause the asymmetric deformation of the contact line and, therefore, the horizontal force that will drive the particles towards the center of the drop [Fig. 5(c), center].

In conclusion, the use of long-range electrostatic forces in the assembly of objects is advantageous as compared to nonspecific interactions induced by gravity or short-range interactions such as hydrogen or covalent bonds. Because of the opportunities offered by μCP to define the chemical functionality and thus surface charge over large areas, the electrostatic forces can be easily manipulated on a micron scale to induce the localized colloidal deposition. An additional in-plane ordering of the adsorbed particles can be further initiated by lateral immersion capillary forces that originate from wetting/dewetting properties of a μ-patterned substrate and colloidal particles. The deposition of colloids on μ-patterned ionic SAMs is, therefore, a simple and convenient route to directing the colloidal assembly into ordered, complex structures in large arrays.

We acknowledge fruitful discussions with Dr. B. I. Shraiman, Professor C. A. Mirkin, and V. Tohver.

*Current address: University of Illinois, Urbana, IL 61801.

[1] A. van Blaaderen, R. Ruel, and P. Wiltzius, Nature (London) **385**, 321 (1997).
[2] R. Singhvi *et al.*, Science **264**, 696 (1994).
[3] C. B. Roxlo *et al.*, Science **235**, 1629 (1987); S. Hayashi *et al.*, J. Colloid Interface Sci. **144**, 538 (1991); F. Burmeister *et al.*, Langmuir **13**, 2983 (1997).
[4] B. Russel, D. A. Saville, and W. R. Schowalter, *Colloidal Dispersions* (Cambridge University Press, Cambridge, England, 1989); T. A. Witten, Rev. Mod. Phys. **71**, S367 (1999); S. Giasson, D. A. Weitz, and J. N. Israelachvili, Colloid Polym. Sci. **277**, 403 (1999).
[5] N. D. Denkov *et al.*, Langmuir **8**, 3183 (1992).
[6] K. U. Fulda and B. Tieke, Adv. Mater. **6**, 288 (1994); S. Rakers, L. F. Chi, and H. Fuchs, Langmuir **13**, 7121 (1997); L. N. Donselaar, A. P. Philipse, and J. Suurmond, Langmuir **13**, 6018 (1997); S. H. Park, D. Qin, and Y. Xia, Adv. Mater. **10**, 1028 (1998).
[7] M. Trau, D. A. Saville, and I. A. Aksay, Science **272**, 706 (1996); S. R. Yeh, M. Seul, and B. I. Shraiman, Nature (London) **386**, 57 (1997).
[8] M. M. Burns, J.-M. Fournier, and J. A. Golovchenko, Science **249**, 749 (1990).
[9] C. A. Murray and D. H. van Winkle, Phys. Rev. Lett. **58**, 1200 (1987); A. E. Larsen and D. G. Grier, Nature (London) **385**, 230 (1997).
[10] A. Kumar and G. M. Whitesides, Appl. Phys. Lett. **63**, 2002 (1993); A. Kumar *et al.*, Acc. Chem. Res. **28**, 219 (1995).
[11] J. Aizenberg, A. J. Black, and G. M. Whitesides, Nature (London) **398**, 495 (1999); V. K. Gupta and N. L. Abbott, Science **276**, 1533 (1997); J. Tien, A. Terfort, and G. M. Whitesides, Langmuir **13**, 5349 (1997); J. Aizenberg, A. J. Black, and G. M. Whitesides, Nature (London) **394**, 868 (1998).
[12] J. N. Israelachvili, *Intermolecular and Surface Forces* (Academic Press, London, 1991).
[13] G. M. Bell, S. Levine, and L. N. McCartney, J. Colloid Interface Sci. **33**, 335 (1970).
[14] R. J. Hunter, *Zeta Potential in Colloid Science* (Academic Press, London, 1981).
[15] N. B. Larsen *et al.*, J. Am. Chem. Soc. **119**, 3017 (1997).